

# Lawrence Berkeley National Laboratory

## Lawrence Berkeley National Laboratory

**Title**

STRESS MEASUREMENTS IN THE STRIPA GRANITE

**Permalink**

<https://escholarship.org/uc/item/2rd20165>

**Author**

Carlsson, H.

**Publication Date**

1978-08-01

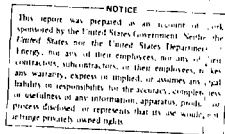
STRESS MEASUREMENTS IN THE STRIPA GRANITE

H. Carlsson

Division of Rock Mechanics  
University of Luleå  
Luleå, Sweden

Reprinted by Lawrence Berkeley Laboratory  
University of California  
Berkeley, California 94720

August, 1978



Originally part of KBS Teknisk Rapport 49, Kärnbränslesäkerhet (KBS)  
(Swedish Nuclear Fuel Safety Program)

August, 1977

## PREFACE

This report is one of a series documenting the results of the Swedish-American cooperative research program in which the cooperating scientists explore the geological, geophysical, hydrological, geochemical, and structural effects anticipated from the use of a large crystalline rock mass as a geologic repository for nuclear waste. This program has been sponsored by the Swedish Nuclear Power Utilities through the Swedish Nuclear Fuel Supply Company (SKBF), and the U.S. Department of Energy (DOE) through the Lawrence Berkeley Laboratory (LBL).

The principal investigators are L.B. Nilsson and O. Degerman for SKBF, and N.G.W. Cook, P.A. Witherspoon, and J.E. Gale for LBL. Other participants will appear as authors of subsequent reports.

Previously published technical reports are listed below.

1. *Swedish-American Cooperative Program on Radioactive Waste Storage in Mined Caverns* by P.A. Witherspoon and O. Degerman. (LBL-7049, SAC-01)
2. *Large Scale Permeability Test of the Granite in the Stripa Mine and Thermal Conductivity Test* by Lars Lundström and Håken Stille. (LBL-7052, SAC-02)
3. *The Mechanical Properties of Stripa Granite* by Graham Swan (LBL-7074, SAC-03)

TABLE OF CONTENTS

|  |    |
|--|----|
| 1. SUMMARY . . . . .                                   | 1  |
| 2. INTRODUCTION. . . . .                               | 1  |
| 3. SHORT DESCRIPTION OF THE MEASURING METHOD . . . . . | 1  |
| 4. LOCATION OF BOREHOLE FOR THE MEASUREMENTS . . . . . | 4  |
| 5. MECHANICAL PROPERTIES OF THE GRANITE . . . . .      | 6  |
| 6. RESULTS FROM THE MEASUREMENTS . . . . .             | 7  |
| 7. COMMENTS ON THE RESULTS . . . . .                   | 11 |
| 8. CORRELATION WITH GEOLOGICAL STRUCTURES . . . . .    | 12 |
| 9. REFERENCES . . . . .                                | 13 |

## 1. SUMMARY

Rock stress measurements at the 348 m level of the Stripa Mine have been carried out with the Leeman tri-axial equipment. The largest principal stress is found to be 20.0 MPa and directed parallel with the strike of the contact between the granite and the orebody. The intermediate principal stress is 11.4 MPa and directed almost horizontal and perpendicular to the contact. The minor principal stress has a magnitude of 5.4 MPa. The deduced vertical stress is approximately of the same value as can be theoretically calculated.

## 2. INTRODUCTION

In order to solve the problems of nuclear waste storage the owners of the nuclear plants in Sweden organized Nuclear Fuel Safety (KBS) in late fall 1976.

Some of the reasearch that KBS performed took place in an abandoned iron ore mine in Stripa, situated in the central part of Sweden. Adjacent to the mine lies a massive body of granite where all experiments have been accomplished.

One of the investigations that took place in the Stripa granite was stress measurements. These have been carried out by the Division of Rock Mechanics, University of Luleå, Sweden.

## 3. SHORT DESCRIPTION OF THE MEASURING METHOD

The method that was used for determination of the stress tensor was the Leeman three-dimensional overcoring method. The method is based upon determination of strain in a borehole by using strain gauges. Twelve strain gauges are divided into three rosettes spaced at an angle of  $120^\circ$  around the

perimeter of an EX drill hole. The layout of the rosette is shown in Fig. 1.

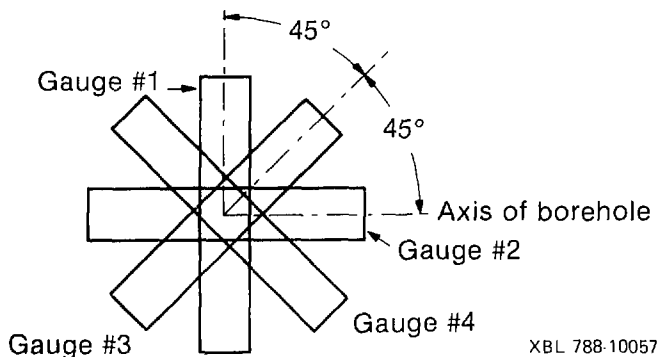
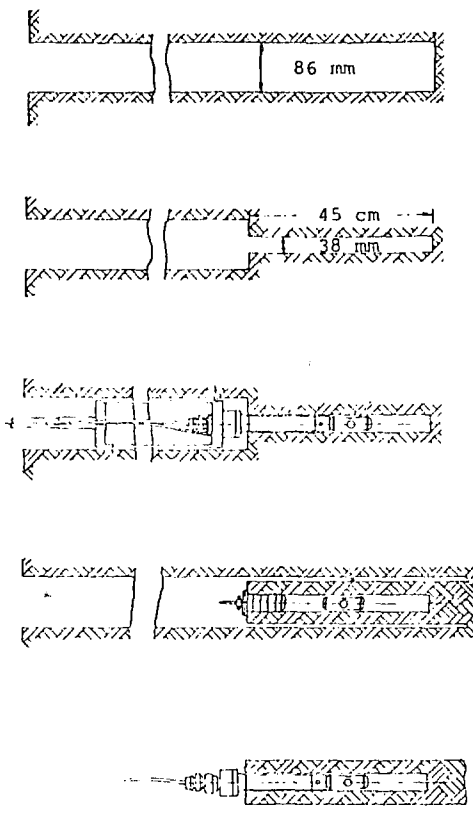


Fig. 1. The strain rosette of a triaxial cell.

In principle, the way of doing the measurements is shown in Fig. 2. An 86-mm borehole is drilled to the required depth. The bottom of the hole is flattened with a full face diamond bit. Concentric with the 86-mm borehole an EX hole (38 mm) is drilled for a distance of 45 cm. After the hole is cleaned, a triaxial strain cell with three strain gauge rosettes is glued in the EX portion of the hole. After the glue has hardened and stable readings of the strain gauges have been recorded, the EX hole is plugged and a cylinder is overcored, as shown in Fig. 2d. The cylinder is then removed from the borehole and the strain obtained is recorded by reading the 12 strain gauges.

In each measuring location the stress tensor can be determined by knowing the Young's Modulus and Poisson's Ratio of the rock. These properties are determined from the core associated with each measuring location in the borehole.

In order to check the reliability of the gauge readings, the overcored cylinder with the bounded triaxial cell is carefully tested in the laboratory.

- 
- a) The borehole is drilled into the rock mass to the point where the stress in the rock is to be measured.
- b) A pilot hole 45 cm long is drilled into the end of and concentric with the main borehole.
- c) After cleaning and drying of the pilot hole, the triaxial cell is inserted and the strain gauges are glued. When the glue has set, strain readings are taken.
- d) The pilot hole is plugged and the triaxial cell is overcored.
- e) The core is broken at the end of the borehole and stress-relieved strain readings are taken.

XBL 788-10051

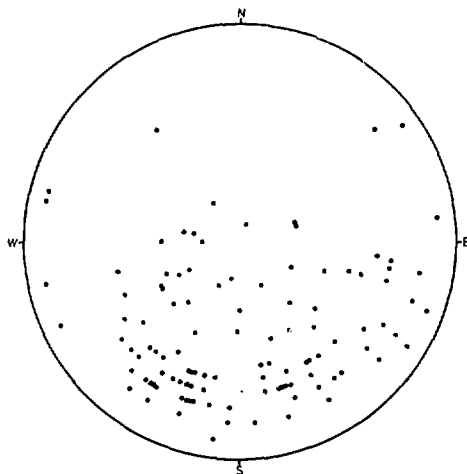
Fig. 2. The principles of rock stress measurements using the overcoring technique. (From Instruction Manual for the use of the C.S.I.R. rock stress measuring equipment.)

#### 4. LOCATION OF BOREHOLE FOR THE MEASUREMENTS

The measurements were carried out in a borehole located in a drift at 348-m level. Determination of direction of the borehole was based upon the strike and dip of visible fractures in the drift. Two dominating sets of fractures were observed. The first set had a strike of N-S and a dip of  $70^{\circ}$  W. The second set had a strike of N69- $70^{\circ}$  E and a dip of  $65^{\circ}$  W. Additional fracture mapping in the main drift of the test site was carried out by SGU (Swedish Geological Survey), as shown in Fig. 3.

XBL 788-10056

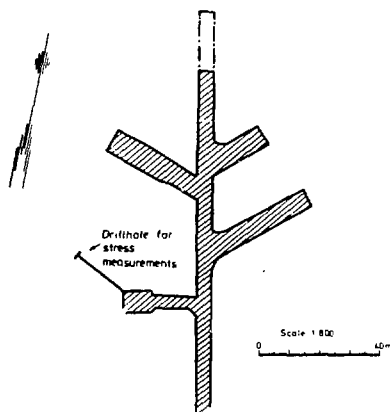
Fig. 3. Stereographic projection of joint surfaces from the main drift of the test site. Data from Olkiewicz, 1977.



The effort was then made to orient the borehole so that no axial fractures would appear in the core, since this would have affected the continuity of the measurements. A diabase dike in the end of the drift also contributed



to determining the direction of the borehole. The same dike is observed elsewhere in the mine, and has a width varying between 1.5-2.0 m. The decision was made to drill through the dike and start the measurements at the location in the borehole where the virgin stresses were not affected by the dike. The test site and the direction of the borehole are shown in Fig. 4.



XBL 783-10055

Fig. 4. Location of rock stress measurements at the 348 m level.

The results from the stress measurements were intended to be used for the purpose of orienting the boreholes in a heater test to be accomplished in the same drift. In order to get a satisfactory and reliable determination of the stress tensor in the granite, the measurements were carried out at a great number of locations in the borehole.

## 5. MECHANICAL PROPERTIES OF THE GRANITE

For the computation of the stress tensor, Young's Modulus and Poisson's Ratio have to be known. These parameters have been determined from cores sampled in association with the strain measurement locations in the borehole. The cores have a diameter of 72 mm and a length of 180 mm, i.e.,  $l/d = 2.5$ . The determined parameters are tabled below. The values are secant values at 50% failure load.

| Depth<br>[m] | Young's Modulus<br>[GPa] | Poisson's Ratio<br>$\nu$ | Failure load<br>[MPa] |
|--------------|--------------------------|--------------------------|-----------------------|
| 6.03         | 59.97                    | 0.19                     | 151.39                |
| 7.68         | 56.46                    | 0.17                     | 140.40                |
| 8.53         | 59.94                    | 0.19                     | 152.50                |
| 10.10        | 61.68                    | 0.22                     | 141.40                |
| 11.44        | 59.06                    | 0.19                     | 154.70                |
| $\bar{m}$    | 59.42                    | 0.192                    | 148.01                |

As shown in the table, the variation between Young's Modulus and Poisson's Ratio is very small. The decision was made to use  $E = 59.42$  GPa and  $\nu = 0.192$  for all computations, since a minor change in these parameters has almost no effect on the magnitudes and no effect on the directions of the stresses.

## 6. RESULTS FROM THE MEASUREMENTS

The stress tensor has been determined at 19 locations along a 20-m-long subhorizontal borehole at the 348 m level. As mentioned earlier, the borehole was drilled through a diabase intercept which ended after 0.87 m. In order to check the influence of the dike on the stresses in the granite, the first measuring location was placed at a depth of 1.55 m in the borehole. Unfortunately, the diabase again occurs at 2.05 m. At 2.87 m the diabase ends and the granite persists throughout the remainder of the borehole. Close to the dike the granite was highly fractured, which made it impossible to perform any measurements. As a result of this the second strain measurement was located at 4.41 m. The last strain measurement was located at a depth of 19.63 m.

Table I shows the measured strain for each gauge at each location in the borehole. Table II shows the calculated principal stresses for each location. In Fig. 5 the principal stresses are plotted as a function of depth of the borehole. The orientation of the principal stresses is shown in Fig. 6.

Table I. Strain measurements from each data point. A Young's Modulus of 59.42 GPa and Poisson's Ratio of 0.192 were used in the calculations.

| Depth<br>[mi] | Strain       |              |              |              |              |              |              |              |              |                 |                 |                 |
|---------------|--------------|--------------|--------------|--------------|--------------|--------------|--------------|--------------|--------------|-----------------|-----------------|-----------------|
|               | $\epsilon_1$ | $\epsilon_2$ | $\epsilon_3$ | $\epsilon_4$ | $\epsilon_5$ | $\epsilon_6$ | $\epsilon_7$ | $\epsilon_8$ | $\epsilon_9$ | $\epsilon_{10}$ | $\epsilon_{11}$ | $\epsilon_{12}$ |
| 1.55          | 148          | 126          | 333          | -50          | 47           | 103          | 185          | -2           | 325          | 118             | 19              | 410             |
| 4.41          | 111          | 74           | 136          | 93           | -20          | 103          | 187          | 123          | 426          | 190             | 100             | 426             |
| 6.03          | 236          | 124          | 253          | -3           | -143         | 54           | 60           | 158          | 369          | 158             | -6              | 505             |
| 6.53          | 263          | 75           | 463          | -35          | -136         | 179          | 130          | -17          | 265          | 152             | 0               | 398             |
| 7.68          | 100          | 52           | 267          | -113         | 75           | 155          | 262          | -7           | 639          | 178             | 61              | 686             |
| 8.53          | 253          | 243          | 405          | 109          | -168         | 239          | 72           | 18           | 493          | 197             | 164             | 472             |
| 9.08          | 39           | 267          | 114          | 191          | 38           | 247          | 296          | 23           | 1911         | 392             | 497             | 870             |
| 9.60          | 96           | 188          | 335          | -34          | 82           | 175          | 250          | 8            | 713          | 188             | 182             | 797             |
| 10.93         | 278          | 200          | 401          | 87           | -7           | 220          | 155          | 39           | 1163         | 226             | 475             | 910             |
| 11.44         | 235          | 176          | 400          | 35           | 230          | 272          | 475          | 35           | 977          | 217             | 212             | 998             |
| 12.22         | 405          | 100          | 496          | 65           | -44          | 95           | 121          | -72          | 1181         | 60              | 355             | 915             |
| 13.31         | 281          | 67           | 217          | 122          | 10           | 49           | 78           | -32          | 255          | 59              | 31              | 298             |
| 13.87         | 248          | 181          | 136          | 236          | 54           | 241          | 235          | 88           | 443          | 234             | 293             | 388             |
| 14.37         | 165          | 236          | 169          | 199          | 222          | 114          | 272          | 69           | 636          | 99              | 233             | 480             |
| 15.43         | 43           | 144          | 183          | 16           | 141          | 188          | 233          | 41           | 488          | 158             | 110             | 512             |
| 16.54         | 164          | 48           | 185          | 29           | 538          | 60           | 328          | 239          | 1057         | 132             | 528             | 708             |
| 17.02         | 410          | 18           | 161          | 310          | -84          | 82           | 80           | -38          | 482          | 61              | 198             | 350             |
| 17.83         | 523          | -43          | 148          | 340          | -69          | 61           | 39           | -42          | 843          | 9               | 457             | 376             |
| 19.63         | -19          | 34           | 0            | 33           | 234          | 44           | 261          | 10           | 558          | 74              | 182             | 371             |

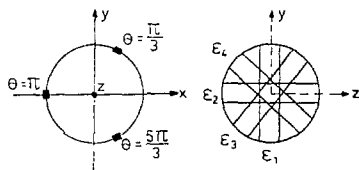
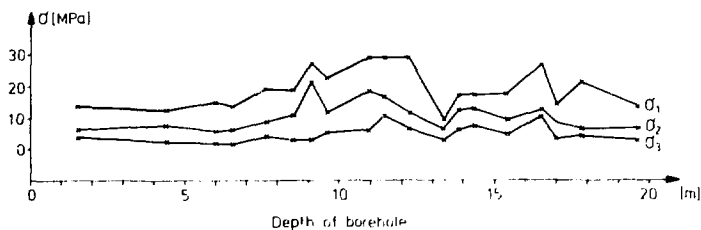


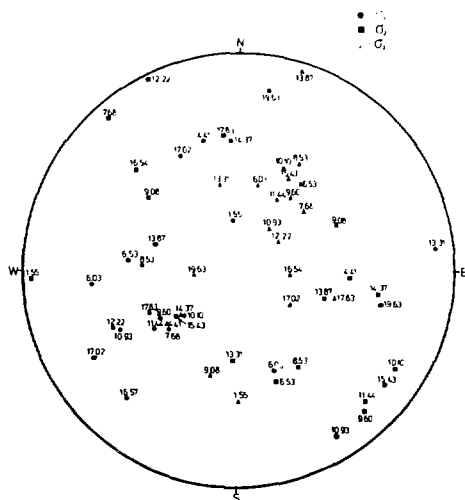
Table 11. Calculated principal stresses.

| Layer<br>No. | Principal stresses |            |            | Vertical comp.<br>[MPa] | Secondary normal<br>principal stresses |       |
|--------------|--------------------|------------|------------|-------------------------|--|-------|
|              | [MPa]              |            |            |                         | [MPa]                                  |       |
|              | $\sigma_1$         | $\sigma_2$ | $\sigma_3$ |                         | A                                      | B     |
| 1.55         | 13.46              | 6.08       | 1.92       | 13.58                   | 6.16                                   | 5.26  |
| 4.41         | 12.28              | 7.98       | 2.22       | 6.02                    | 11.26                                  | 5.44  |
| 6.53         | 15.00              | 5.50       | 1.80       | 4.80                    | 13.20                                  | 4.04  |
| 6.73         | 13.86              | 5.26       | 1.88       | 6.94                    | 16.24                                  | 4.82  |
| 7.68         | 19.36              | 8.44       | 4.04       | 11.56                   | 13.80                                  | 8.40  |
| 8.53         | 18.58              | 10.84      | 3.16       | 12.22                   | 14.4                                   | 7.76  |
| 9.08         | 22.28              | 21.38      | 3.48       | 17.20                   | 23.00                                  | 15.20 |
| 9.60         | 23.06              | 12.26      | 5.18       | 14.04                   | 25.92                                  | 11.47 |
| 10.93        | 28.96              | 18.30      | 6.10       | 10.62                   | 24.64                                  | 18.10 |
| 11.44        | 29.80              | 16.88      | 10.40      | 18.26                   | 22.50                                  | 17.26 |
| 12.22        | 29.52              | 13.74      | 6.88       | 10.68                   | 27.60                                  | 11.76 |
| 13.31        | 9.78               | 6.44       | 3.28       | 4.82                    | 9.87                                   | 4.80  |
| 13.87        | 16.96              | 12.30      | 5.62       | 14.62                   | 14.65                                  | 5.63  |
| 14.37        | 17.36              | 13.14      | 7.26       | 10.48                   | 15.75                                  | 11.51 |
| 15.43        | 16.60              | 9.42       | 4.42       | 11.74                   | 10.62                                  | 8.08  |
| 16.54        | 27.5               | 12.68      | 10.30      | 11.56                   | 26.70                                  | 12.21 |
| 17.02        | 14.18              | 8.70       | 3.30       | 5.98                    | 11.85                                  | 8.34  |
| 17.83        | 21.58              | 6.48       | 4.08       | 11.62                   | 14.68                                  | 5.86  |
| 19.63        | 13.94              | 6.98       | 2.78       | 3.70                    | 13.64                                  | 6.36  |



XBL 788 10054

Fig. 5. Variation of principal stresses in the borehole.



XBL 788-10053

Fig. 6. Direction of principal stresses at each measure point plotted. Depth of measurement in the borehole is indicated on Wulff's net lower hemisphere.

## 7. COMMENTS ON THE RESULTS

In spite of the fact that there is a fairly wide scattering of the orientation of the principal stresses, there is a maximum of  $\sigma_1$  with a dip of approximately  $40^\circ$  in the direction of  $S60^\circ W$ . The corresponding maximum for  $\sigma_3$  is a dip of approximately  $50^\circ$  in the direction of  $N40^\circ E$ . The medium principal stress is more or less horizontal. The location of these measurements is in the interval 6.03-16.53, i.e., well spread along the borehole.

The mean value of the magnitude and orientation of the principal stresses has been calculated within the interval 6.03-16.53 m. The computed principal stresses have been calculated from the mean value of gauges 1, 2, 3 ..... 12 along the borehole. The result, which is plotted in Fig. 7, shows that the maximum principal stress  $\sigma_1$  has the magnitude 20 MPa and is oriented with a dip of  $31^\circ$  in the direction  $S68^\circ W$ .

XBL 788-10052

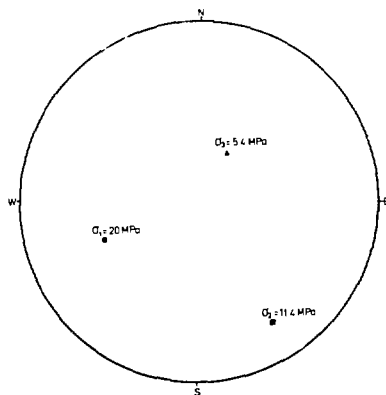


Fig. 7. Principal stresses and their directions for the test site, Stripa mine, 348 m level.

The medium principal stress  $\sigma_2$  has been computed to 11.4 MPa and with a dip of  $13^\circ$  in the direction of  $52^\circ$  E. The minimum principal stress  $\sigma_3$  has the magnitude 5.4 MPa and a dip of  $56^\circ$  in the direction of  $112^\circ$  E.

The measured vertical stress is 9.8 MPa. An overburden of 346 m and a density of 2.7 give a theoretical value of 9.40 MPa, i.e., the deduced vertical component is within 4% of the theoretically derived value.

The biaxial horizontal components,  $\sigma_A$  and  $\sigma_B$ , of the principal stresses have also been computed. These are called "secondary horizontal principal stresses" and are listed in Table II. The mean value for  $\sigma_A$  is 15.58 MPa; and for  $\sigma_B$ , 3.64 MPa.

#### B. CORRELATION WITH GEOLOGICAL STRUCTURES

Unfortunately very little has been published about the geology and especially the tectonic features of the rocks in the Stripa area.

The regional and mine maps show that the rocks are striking in a NE direction and are steeply dipping towards SE. The ore that was mined at Stripa was a quartz-banded iron ore. The main ore had the appearance of a folded disc and the strike was approximately NE. Close to the surface the ore was steeply dipping towards SE, but in deeper regions the dip was very shallow. Bordering the ore was a leptite and a serotogenic granite in which the stress measurements took place. The shallow dip of the ore at deeper regions is believed to be caused by the intrusion of the granite.

The contacts between the rocks undulate both within and between different levels in the mine. At the 348-m level where the measurements were carried out, a strike of  $N45^\circ E$  can be observed; and the distance to the contact between the granite and the ore is approximately 100 m.



The main principal stress  $\sigma_1$  is measured to be 20 MPa, and the orientation is more or less parallel to the strike of the granite. The medium principal stress,  $\sigma_2$ , which has been measured to be 11.4 MPa, has a subhorizontal orientation and the direction is almost perpendicular to the contact of the granite.

It is not certain that the calculated stress tensor is the same for the granite intrusion as a whole. Faults and folds which have a general appearance in the Stripa granite disturb the stress field. The only way to get a more detailed picture of the stress tensor in the Stripa granite is to do more measurements at suitable locations in the area.

## 9. REFERENCES

- Denkhaus, H. G., Instruction Manual for the Use of the C.S.I.R. Triaxial Rock Stress Measuring Equipment. C.S.I.R. - Report MWF 4401, Pretoria 1973.
- Olkiewicz, A., Personal communication. Swedish Geological Survey, 1977.